Hardware Demonstration of Weak Grid Oscillations in Grid-Following Converters

Li Bao, Lingling Fan, Zhixin Miao, Zhengyu Wang
Department of Electrical Engineering
University of South Florida
{libao, linglingfan, zmiao, zhengyuwang}@usf.edu

***Abstract*—The increasing penetration of inverter-based resources (IBRs) introduces some unexpected dynamic issues, including low-frequency oscillations. In this paper, a laboratory-scale grid-following voltage-source converter (VSC) system is implemented to demonstrate weak grid oscillations. Grid-following control is applied in VSC to provide active power, reactive power or ac voltage control. The test bed is also replicated in electromagnetic transient (EMT) simulation environment (MATLAB/SimPowerSystems) for benchmark purpose. Case studies are carried out to demonstrate low-frequency oscillations under real power/ac voltage or real power/reactive power control. The excellent agreement between the simulation and experimental results ensures that the two test beds are exchangeable and can be used for testing oscillation mitigation strategies in future research.**

***Index Terms*—Three-phase VSC, vector control, laboratory test bed**

I. Introduction

Power electronic converters are now widely used in generation, transmission, and distribution systems [1]. Three-phase VSCs have been the key components in high-voltage direct-current (HVDC) transmission systems, machine drives, and flexible AC transmission systems (FACTS) [2], [3]. In addition, they serve as the interface of wind and solar photovoltaics (PV) grid integration [4–6]. Converter-driven stability issues have been identified by a recent IEEE PES Taskforce paper [7] as the newly emerging stability issues in power grids. This paper focuses on low-frequency oscillation stability issues of IBRs in weak grids.

Currently, the majority of wind and solar PVs adopt grid-following control strategy for the grid-connected VSCs. Operating in weak grids has been identified as a critical challenge for grid-following converter-interfaced IBRs by the grid industry worldwide, e.g., North American Electric Reliability Corporation (NERC) [8] and Australian Energy Market Operator (AEMO) [9]. Specifically, weak grid oscillation is an issue that has been observed in real world. Weak grid oscillation events in wind farms have been documented in IEEE PES TR-80 "Wind Energy Systems Subsynchronous Oscillations: Events and Modeling" [10]. In addition, NERC has documented several wind farm and solar PV low-frequency oscillation events due to weak grid operation from 2010-2016 [11].

This issue of low-frequency oscillations due to IBRs in weak grids has been studied by the senior authors, e.g., in [12–15]. While the senior authors have conducted preliminary research on mechanism and mitigation strategy of weak grid oscillations for grid-following converters in [12–15], the study scope is limited to grid-following converters with ac voltage control and the validation is limited to computer simulation.

Many other possible control structures, e.g., reactive power control mode, volt-var droop control, have not been considered in the prior research. In addition, results from hardware test beds are desired to provide an additional layer of verification.

The objective of this paper is to demonstrate weak grid low-frequency oscillations of a grid-connected VSC system with ac voltage control or var control in both hardware and simulation. This is the first step of an overall research goal that aims to develop a stability enhancement strategy and validate the strategy through hardware experiments for technology readiness.

A hardware test bed consisting of a SiC VSC, a 45-kW Chroma grid simulator, and passive components such as resistors, inductors, and capacitors, has been built to represent an IBR with weak grid interconnection. A corresponding EMT test bed is built in MATLAB/SimPowerSystems. This computer simulation test bed is developed to mirror the laboratory test bed except that the VSC assumes average model without the 5-kHz pulse width modulation switching details to save computing time.

Different control methods such as P/Q and P/V control are utilized to examine the active power exporting limit and oscillations. Results show that oscillations can be observed in a P/V control system regardless controller parameters. By contrast, the P/Q control system experiences oscillations only under specific parameters.

The structure of this paper is organized as follows. In Section II, the configuration of the test bed and the parameters are presented. Section III presents the simulation test bed and the hardware test bed setup. Section IV presents four case studies implemented in experiments and simulation. The results from the two test beds are compared side by side. Finally, Section V concludes the paper.

This project is supported in part by US Department of Energy grant DE-EE-0008771. The authors would like to acknowledge US Department of Energy Solar Energy Technology Office.

II. Description of the System

The test system is a three-phase VSC connected to a grid through a transmission line. The parameters of the circuit and the VSC's control system are presented in Fig. 1. The power direction and corresponding variables are also illustrated in this figure. R_1 and L_1 represent the choke filter impedance, C_f is the filter capacitor, R_g and L_g are the grid transmission line impedance, P and Q are the active and reactive power from the VSC to the grid, v_a, v_b and v_c represent the three-phase voltage of PCC bus. A PLL is used to synchronize the VSC by tracking the PCC voltage.

The vector control of the VSC is implemented in a synchronous dq frame, which converts time-variant three-phase variables to dc time-invariant values at steady state. Two cascaded loops are included in the control system based on the dq-variants. Inner loop controls currents in dq-frame and outer loop controls P and Q (or the PCC voltage V). The PLL provides an angle θ for the abc to dq conversion. At steady state, the d-axis PCC voltage v_d is aligned to the PCC voltage space vector and the q-axis PCC voltage v_q is kept as zero. The active power and reactive power can be expressed in equation (1).

$$P = v_d i_d + v_q i_q, \;\; Q = v_q i_d - v_d i_q \tag{1}$$

Since v_q is controlled as zero, it can be concluded that P and Q are directly proportional to i_d and i_q, respectively. Therefore, the inner-loop reference i_d^* and i_q^* are generated from outer-loop P control and Q control. Then (1) can be simplified as the follows:

$$\begin{aligned} P &= v_d i_d, \\ Q &= -v_d i_q. \end{aligned} \tag{2}$$

Similarly, as V control is related to Q control, the above analysis is also applicable when the outer loop is P/V control. Parameters of the circuit are listed in Table I .

TABLE I: Parameters of the circuit

Description	Parameters	Values (SI)
Power base	S_b	50 W
System frequency	f	60 Hz
Voltage base (L-L RMS)	V_b	20 V
Grid voltage (Phase RMS)	V_s	11.5 V
DC voltage	V_{dc}	40 V
Switching frequency	f_s	5 kHz
Converter filter	R_1	0.27 Ohm
	L_1	1.5 mH
Transmission line	R_g	0.76 Ohm
	L_g	9.7 mH
PLL	k_{pPLL}, k_{iPLL}	60, 1400

The parameters of control system are listed in Table II. Two groups of parameters with different bandwidths will be investigated.

III. Test Beds in Hardware and Simulation

A. Hardware test bed

The VSC system shown in Fig. 1 has been set up in an experimental test bed. Fig. 2 shows the setup of the experiment

TABLE II: Parameters of the controller

	Control loop	Parameters	Bandwidth (Hz)
Parameters I	Current control	k_{pi}=1, k_{ii}=10	118.9
	P control	k_{pp}=0.25, k_{ip}=25	3.3
	Q or V control	k_{pq}=0.25, k_{iq}=25	3.3
Parameters II	Current control	k_{pi}=0.4758, k_{ii}=3.28	48.0
	P control	k_{pp}=0.25, k_{ip}=25	3.3
	Q or V control	k_{pq}=1.1, k_{iq}=137.5	15.5

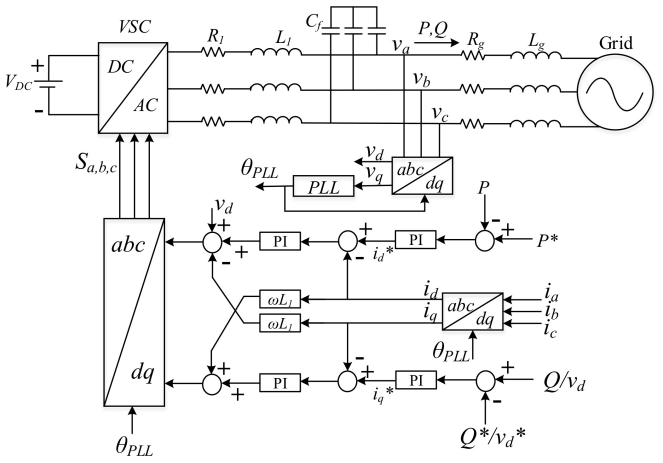

Fig. 1: Configuration of grid-connected three-phase VSC and its control system.

test bed. A three-phase VSC is built by a three-pack Imperix PEB-8024 half-bridge SiC module with maximum 800 V DC voltage, 24 A output current, and 200 kHz switching frequency. Each Imperix pack includes an embedded current sensor with a 280-kHz bandwidth.

A Chroma grid simulator 61845 behaves as a grid emulator. It is a bidirectional single- and three-phase power supply. So the power generated by VSC can be sent into the grid emulator. The PCC voltage is measured by an OPAL-RT OP8662 high voltage and current probe, which has up to 600-V input range and 100-kHz bandwidth.

The signal processing and control system are implemented in a Real-Time simulator RT-Lab OP5600. The current measurements from the Imperix module and the voltage measurements from OPAL-RT OP8662 are all sent back to RT-Lab for processing and recording. The processing and control model are firstly built in MATLAB/SimPowerSystems, then converted to C code and implemented in RT-Lab. A typical RT-Lab model consists of two subsystems as the master and the console. The master subsystem includes the computational and control part. For example, the vector control and power calculation are assigned to the master subsystem. The console subsystem is used to observe the measured and calculated signals, switch Q or V control, and adjust active power reference value in real time.

After processing these data, six PWM signals will be generated by the RT-Lab and sent to VSC's gates through an Imperix OPAL-RT to Power Modules interface.

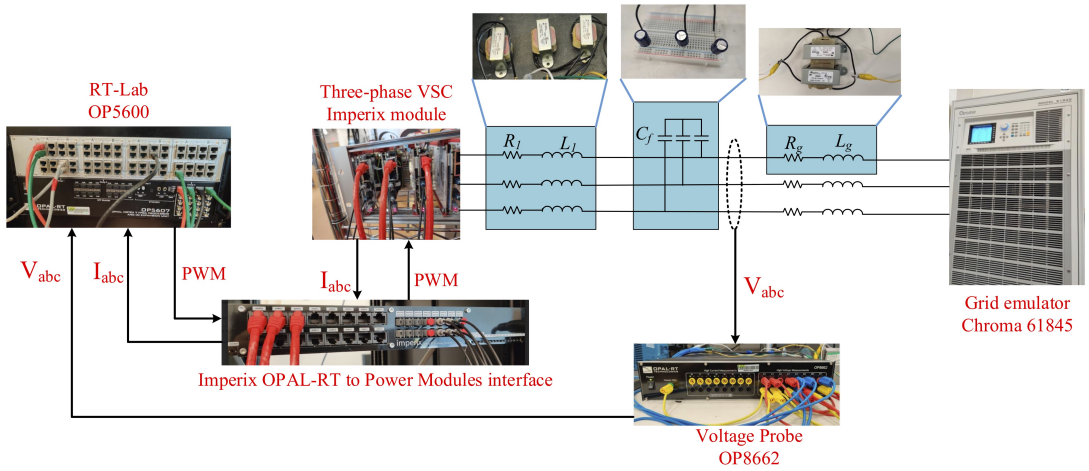

Fig. 2: Configuration of the hardware test bed.

B. Simulation test bed

The VSC system shown in Fig. 1 is simulated in MATLAB/SimPowerSystems software. Both control system and power circuit components are created using the blocks in the library. The VSC block is an average model, which uses a reference signal u_{ref} to represent the output terminal voltage v_{abc}, so the controlled signal of VSC block is a three-phase sinusoidal waveform instead of PWM signal. This model does not contain harmonics and has a faster simulation speed. A switch is used in q-axis outer loop to choose Q or V control manually. The time step is set as 25 μs. Fig. 3 shows the simulation model. It should be noticed that the calculation process for P and Q, filter, and dq-axis decoupled process are not shown.

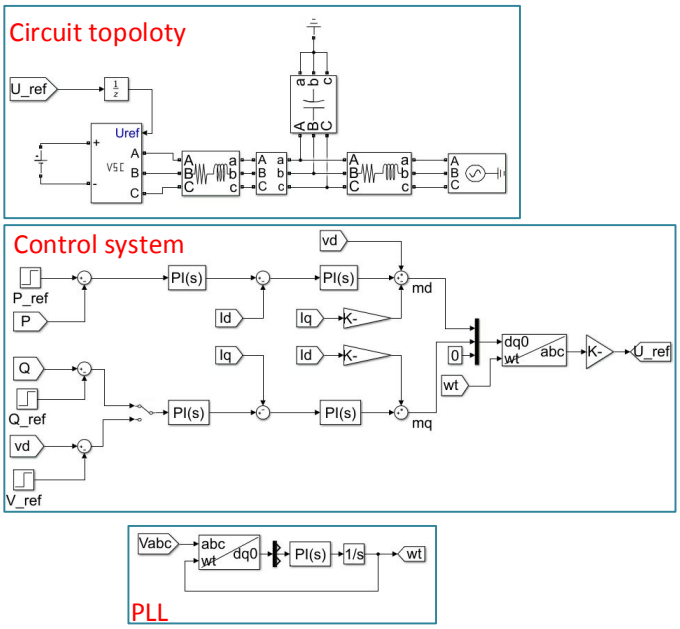

Fig. 3: Configuration of the MATLAB/SimPowerSystems model.

C. Lessons learned in benchmarking

Benchmarking the computer simulation test bed and the hardware test bed is a time-consuming task. It requires attention to meticulous details. Three lessons have been learned in this process.

- Per-unit calculation for simulation and experiment requires attention. In this research, the grid-following converter control parameters, e.g., current control, outer controls, and PLL, are all in per unit values. This requires that the measurements are all converted to per unit values. In the computer simulation test bed, the per-unit calculation is realized automatically by the three-phase measurement block in the SimPowerSystems model, where the nominal voltage is the line-to-line RMS value as 20 V. On the other hand, in the hardware test bed, real-time three-phase voltage signals are measured and sent to RT-Lab for processing. Per unit calculation is followed. The base for the instantaneous voltage signals is different from the RMS value, rather, the per-phase peak value 16.3 V or $\sqrt{\frac{2}{3}} \times 20$ V should be used.
- The value of an inductor's inductance should be carefully measured. The inductance has mismatch from the value in an inductor's label. In this research, the inductor's label shows it has inductance of 15 mH at 4 A. According to experimental results and steady-state calculation, the circuit current is about 2 A in this case. Moreover, since the inductance is too large for this system, two inductors are connected in parallel so the transmission line impedance is reduced, which means that the current through each inductor is also changed to half. Under this operation condition, the circuit current is lower than the rated current, this change also influences the inductance value. To find the accurate inductance, the Chroma 61485 grid simulator is connected to the inductor directly and operates at the desired operation condition. By measuring the voltage across the inductor and its current, the inductance can be calculated as about 9.7 mH (parallel

connection) when working at this current. This value is then used in simulation fro verification.

- PWM signals generation in the hardware test bed needs attention. The hardware test bed employs RT-Lab to implement control algorithm. The output PWM signals are defined by the duty ratio d, not PWM's modulation index m. On the other hand, the output of vector control system is the reference voltage u_{ref}. The equation to convert u_{ref} to d is as follows:

$$d = \frac{1}{2}(u_{\text{ref}} + 1).$$

IV. Case studies

In order to investigate the oscillation characteristics, four case studies are presented. All case studies are first conducted in the hardware test bed, then benchmarked in the simulation test bed. Different control strategies and parameters are examined and compared. For each case, active power is given a step change to reach marginal stability condition. P, Q from VSC and PCC bus V are presented. The experimental data are collected from RT-Lab and plotted by MATLAB. Both simulations and hardware experiments have the same parameters. Results from two models are compared for verification.

A. P/Q control with Parameters I

In this case, the VSC is operated in P/Q control mode with parameters listed in Table II. Both experimental model and simulation are working at steady-state when P is set as 1.65 pu.

Figs. 4a and 4b present the measurements taken from the hardware test bed and the simulation test bed: P, Q exports from the VSC to the PCC bus. Q is regulated as 0.2 pu, and when P is increased to 1.68 pu, the measurements from the experiment test bed shows the system has voltage collapse. For the simulation model, voltage collapse occurs when P increases to 1.7 pu.

Before the step change of P, the PCC bus voltages are 1 pu for both models, which demonstrates a good agreement.

B. P/Q control with Parameters II

In previous case, the system is collapsed without any oscillation when P increases to the marginal stability condition. On the other hand, with Parameters II, oscillations can be observed. Figs. 4c and 4d present the measurements from the hardware test bed and the simulation test bed. Both test beds show oscillations and the system becomes unstable if the real power exporting level increases.

In this case, Q is still controlled as 0.2 pu while P is at 1.58 pu at steady-state. When P is increased to 1.61 pu in the experiment test bed, an undamped 3-Hz oscillation appears. In simulation model, a 3-Hz oscillation is also observed when P increases to 1.65 pu. At steady-state, since P and Q are controlled at the same level for both test beds, the PCC voltages of the two test beds are found to be same at 1.05 pu.

C. P/V control with Parameters I

Under the P/V control, the PCC voltage is kept as 1 pu. The dynamic responses are shown in Figs. 5a and 5b. The initial value of power is 1.92 pu for both hardware and simulation test beds. It can be seen that when P reaches 1.94 pu, the measurements from the experiment test bed show that the system becomes unstable and the frequency of the oscillation is 2.8 Hz. In the simulation model, a 2.8-Hz oscillation also appears when P changes to 1.97 pu.

At steady-state before step change, the reactive power for both models are 0.42 pu.

D. P/V control with Parameter II

In this case, the VSC applies P/V control with the Parameters II. The results are shown in Figs. 5c and 5d. P has a step change from 1.53 pu, and V is kept as 1 pu. The measurements from the hardware test bed show 3.3-Hz oscillations when P increases to 1.57 pu. In the simulation model, the power limit is 1.59 pu, and the oscillation frequency is also around 3.3 Hz. Before the step change, Q in two models are about 0.19 pu.

E. Summary

Since the laboratory experiment is benchmarked with simulation model built in MATLAB/SimPowerSystems, and operating at the same condition, dynamic simulation results and steady-state values can be used to compare for the same event: a step change in P. Table III summarize these results in digital for a better comparison, which shows excellent matching with only slight difference on the marginal power limits.

V. Conclusion

This paper demonstrates weak grid oscillations of a grid-following VSC system. The VSC system is implemented in a hardware test bed and a computer simulation test bed in MATLAB/SimPowerSystems. Four case studies are carried out under different control methods and different parameters. With the grid-following control, active power is controlled and increased to marginal stability condition. For P/Q control, the oscillation can only be observed with specific parameters. On the other hand, the system with P/V control shows oscillations at marginal stability condition regardless of controller parameters. The response of active power, reactive power and PCC voltage from experiment and simulation are provided and compared. The good agreement of active power exporting limit, oscillation frequency and steady state variables before events demonstrates the accuracy of the computer simulation test bed.

References

[1] Z. Huang, H. Krishnaswami, G. Yuan, and R. Huang, "Ubiquitous power electronics in future power systems: Recommendations to fully utilize fast control capabilities," *IEEE Electrification Magazine*, vol. 8, no. 3, pp. 18–27, 2020.

[2] X. Jiang, X. Fang, J. H. Chow, A.-A. Edris, E. Uzunovic, M. Parisi, and L. Hopkins, "A novel approach for modeling voltage-sourced converter-based facts controllers," *IEEE Transactions on Power Delivery*, vol. 23, no. 4, pp. 2591–2598, 2008.

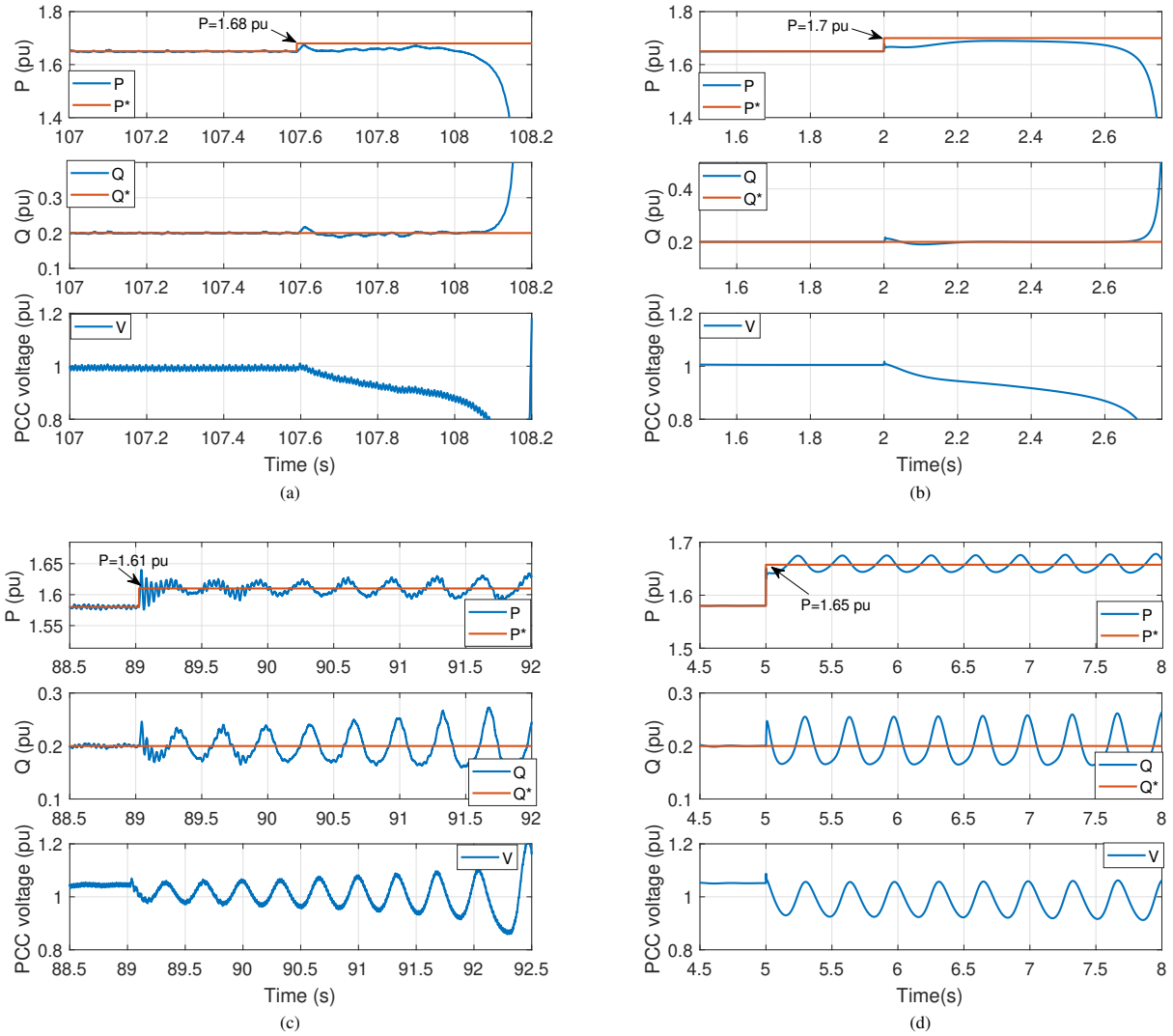

Fig. 4: Response of P, Q and PCC voltage under P/Q control when P is given a step change. Upper row: Parameters I. Lower row: Parameters II. Left column: Experiment results. Right column: Simulation results.

TABLE III: Results comparison

Case studies	Test bed	Power limit (pu)	Oscillation frequency (Hz)	Steady-state value before event		
				P (pu)	Q (pu)	V (pu)
P/Q control with Parameters I	Simulation	1.68	-	1.65	0.2	1
	Experiment	1.70	-	1.65	0.2	1
P/Q control with Parameters II	Simulation	1.61	3	1.58	0.2	1.05
	Experiment	1.66	3	1.58	0.2	1.05
P/V control with Parameter I	Simulation	1.94	2.8	1.92	0.42	1
	Experiment	1.97	2.8	1.92	0.42	1
P/V control with Parameter II	Simulation	1.59	3.3	1.53	0.19	1
	Experiment	1.57	3.3	1.58	0.19	1

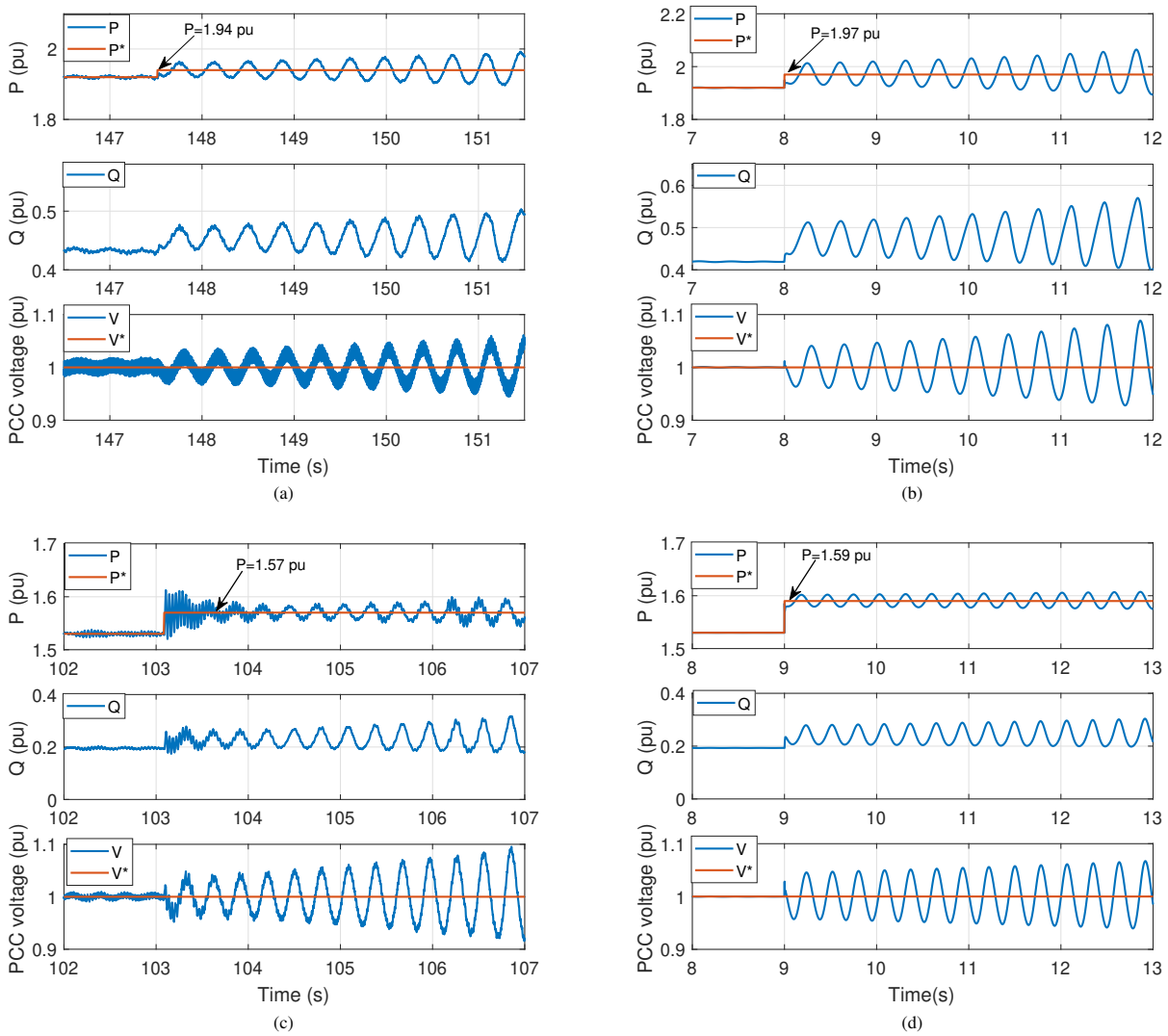

Fig. 5: Response of P, Q and PCC voltage under P/V control with Parameters I or Parameters II when P is subject to a step change. Upper row: Parameter I. Lower row: Parameter II. Left column: Experiment results. Right column: Simulation results.

[3] N. Flourentzou, V. G. Agelidis, and G. D. Demetriades, "Vsc-based hvdc power transmission systems: An overview," *IEEE Transactions on Power Electronics*, vol. 24, no. 3, pp. 592–602, 2009.

[4] G. Reed, R. Pape, and M. Takeda, "Advantages of voltage sourced converter (vsc) based design concepts for facts and hvdc-link applications," in *2003 IEEE Power Engineering Society General Meeting (IEEE Cat. No.03CH37491)*, vol. 3, 2003, pp. 1816–1821 Vol. 3.

[5] B. Wen, D. Dong, D. Boroyevich, R. Burgos, P. Mattavelli, and Z. Shen, "Impedance-based analysis of grid-synchronization stability for three-phase paralleled converters," *IEEE Transactions on Power Electronics*, vol. 31, no. 1, pp. 26–38, 2016.

[6] P. Mitra, L. Zhang, and L. Harnefors, "Offshore wind integration to a weak grid by vsc-hvdc links using power-synchronization control: A case study," *IEEE Transactions on Power Delivery*, vol. 29, no. 1, pp. 453–461, 2014.

[7] N. Hatziargyriou, J. Milanovic, C. Rahmann, V. Ajjarapu, C. Canizares, I. Erlich, D. Hill, I. Hiskens, I. Kamwa, B. Pal *et al.*, "Definition and classification of power system stability revisited & extended," *IEEE Transactions on Power Systems*, 2020.

[8] NERC. (2017, December) Integrating InverterBased Resources into Low Short Circuit Strength Systems: Reliability Guideline .

[9] AEMO. (2020, November) ISystem strength workshop.

[10] IEEE PES WindSSO Taskforce, *PES TR-80: Wind Energy Systems Subsynchronous Oscillations: Events and Modeling*, 2020.

[11] NERC. (2017, September) Reliability Guideline Forced Oscillation Monitoring & Mitigation.

[12] L. Fan and Z. Miao, "An explanation of oscillations due to wind power plants weak grid interconnection," *IEEE Transactions on Sustainable Energy*, vol. 9, no. 1, pp. 488–490, 2018.

[13] Y. Li, L. Fan, and Z. Miao, "Wind in weak grids: Low-frequency oscillations, subsynchronous oscillations, and torsional interactions," *IEEE Transactions on Power Systems*, vol. 35, no. 1, pp. 109–118, 2020.

[14] L. Fan and Z. Miao, "Wind in weak grids: 4 hz or 30 hz oscillations?" *IEEE Transactions on Power Systems*, vol. 33, no. 5, pp. 5803–5804, 2018.

[15] Y. Li, L. Fan, and Z. Miao, "Stability control for wind in weak grids," *IEEE Transactions on Sustainable Energy*, vol. 10, no. 4, pp. 2094–2103, 2019.